

# FSI SIMULATION OF A FLEXIBLE VORTEX GENERATOR AND THE EFFECTS OF VORTICES TO THE HEAT TRANSFER PROCESS

S.S. Dol<sup>1\*</sup>, H.B. Chan<sup>2</sup>, S.K. Wee<sup>3</sup>

<sup>1</sup>Department of Mechanical Engineering, Abu Dhabi University, Abu Dhabi, United Arab Emirates

<sup>2</sup>Department of Mechanical Engineering, Curtin University Malaysia, Miri, Sarawak, Malaysia

<sup>3</sup>Department of Petroleum Engineering, Curtin University Malaysia, Miri, Sarawak, Malaysia

E-mail: sharulshambin.dol@adu.ac.ae

## ABSTRACT

*This work numerically investigated the strength of vortices behind a flexible vortex generator (FVG) by calculating the circulation using Fluid-Structural Interaction (FSI) simulation of RANS (SST)  $k-\omega$  model. The total circulation showed the vortices formed by the FVG was more significant than those originated by the rigid vortex generator (RVG). From the analyses, the case with more significant structural velocity results in a larger shear or circulation. The structural velocity computation proves an excellent consistency with the model predicted values. This has suggested the reliability of the proposed model. Therefore, the performance of FVG in turbulence augmentation has been identified, suggesting enhanced turbulent transport for the greater heat transfer process. Next, the numerical model was extended to examine the heat transfer performance of the FVG. In general, the findings show that the employment of the FVG has a significant positive impact on the heat transfer process in the heat exchanger.*

**Keywords:** CFD, circulation, flexible vortex generator, FSI, heat transfer, turbulence, wakes

## INTRODUCTION

Turbulence is a significant mechanism in promoting mixing, heat and mass transfer rates. Typically, the vortex generator (VG) was used to augment turbulence by disturbing the flow. Such VG is commonly a stationary structure and can be in various shapes and geometries, such as cylinders, winglets or square and triangular blocks. Chan et al. [1] numerically examined the effects of aspect ratio (AR), and geometry have on the flow behaviours of a free end finite cylinder. The circular cantilever cylinder and a rectangular flat plate were applied as the geometry. Velocity defect is larger for a rectangular flat plate than that of a circular cantilever, suggesting larger vortices are present in the wakes of the rectangular flat plate. Their turbulent kinetic energy calculations support the observation. Yong et al. [2] conducted numerous experiments

studying the profiles of the flexible finite cylinder. The velocity field was analyzed, and the turbulence production terms were determined. Their finding demonstrates that the turbulence production term formed from the FVG was, at maximum,  $\sim 2.3$  times of the value generated by its rigid cylinder. They referred to the weakening of downwash (i.e., reduction in vertical velocity component behind the cylinder) as the reason for such augmentation.

Dol et al. [3] numerically investigated the turbulence profiles of the wakes region behind a free-oscillating flexible vortex generator (FVG) by studying the shear rates around the FVG using Fluid-Structural Interaction (FSI) simulation of RANS (SST)  $k-\omega$  model. The FVG geometries were similar to the RVG discussed in Chan et al. [1]. They observed that the wall shear stress formed by the FVG larger than the RVG, which

suggests that the turbulence was more substantial for FVG. The time-series of the wall shear stress was analyzed, and it found that the maximum wall shear stress when the FVG was in motion while the minimum wall shear stress happened when the FVG stopped moving.

The proposed flow model suggests that the increasing wall shear stress is scaled with the structural velocity. It has been observed, in the Dol et al. research [3], that the boundary layer on the FVG surface has a larger shear. In addition, it is also known that the vortex develops when it is fed by the shear (vorticity) in the boundary layer [4]-[7]. With the a larger shear around the FVG, the formed vortices should have a more extensive circulation compared to the RVG and, consequently higher mixing and mass transfer rates. Since the characteristic of the boundary layer actively governs the heat transfer from a solid wall to the fluid, the result suggests that the rate of heat transfer is altered simultaneously. With reference to those findings, since it is known that the heat transfer rate is closely related to turbulence, the previous results suggest that the FVG may be able to improve the heat transfer process as well. Therefore, this work also discusses the extended applications of the FVG on a heat transfer process. The performance of FVG is compared with RVG, which is running in identical flow conditions with the FVG case, to highlight the differences and/or improvement.

**METHODOLOGY**

**Domain and Boundary Conditions**

Figure 1 shows the simulation domain used in this work. The uniform flow was applied to the inlet of the domain. The boundary conditions are listed in Table 1. In the present work, the circular and flat plate cantilever are applied as the VGs. It is important to highlight that the aim of analyzing two geometries was to get more data about its behaviours and physics that could be hidden if only one geometry was investigated. Moreover, Chan et al. [1] show that the turbulence generated by flat plate cantilever is always stronger than circular cantilever, further vindicate that a reasonable quantitative comparison between both geometries will not be the best way to proceed.

**Table 1** Boundary conditions

Surface	Boundary type
Inlet	Velocity Inlet
Outlet	Pressure Outlet
Bottom surface	Non-Slip Wall
Cylinder	Non-Slip Wall; Co-simulation Interface (flexible)
Top surface	Symmetry Plane
Side surfaces	Symmetry Plane

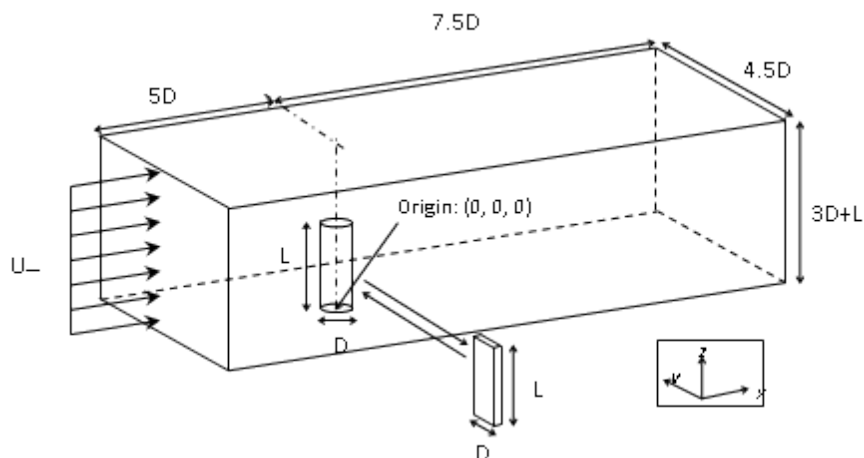


**Figure 1** Schematic of the fluid domain

**Mesh Independency**

Mesh independency analysis was done to achieve the best meshing. The  $y^+$  value was monitored to confirm the near-wall meshes model the boundary layer properly. The details of the meshes used in this work are given in [3]. Figure 2 is the illustration of the optimum mesh setting used in this study.

The coupling between the CFD and FEA to model an FSI problem was also verified by reproducing results obtained by [8]. In this verification, a flexible flat plate cantilever submerged perpendicularly to flow was modelled. The analysis shows that the current model can model an FSI problem with errors that are less than 5% (see [3] for further discussion).

the FVG made from aluminium is highly resistant to deformation due to the high stiffness originating from the material. In order to resolve this issue, the FVG is designed to be long and thin, so that the stiffness ( $k$ ) can be sufficiently reduced. In this case, an  $AR=10$  flat plate cantilever is applied as the VG.

The heat is expected to be convected toward the flow through the vortex formation process: the vortex draws the heat energy from the VG during its formation. Through shedding, the heat is carried away by the vortex. In the wake, the vortex diffuses and stretches that helps to distribute the heat to the colder region. In the case that employs FVG, it is anticipated that the vortex may have drawn more heat

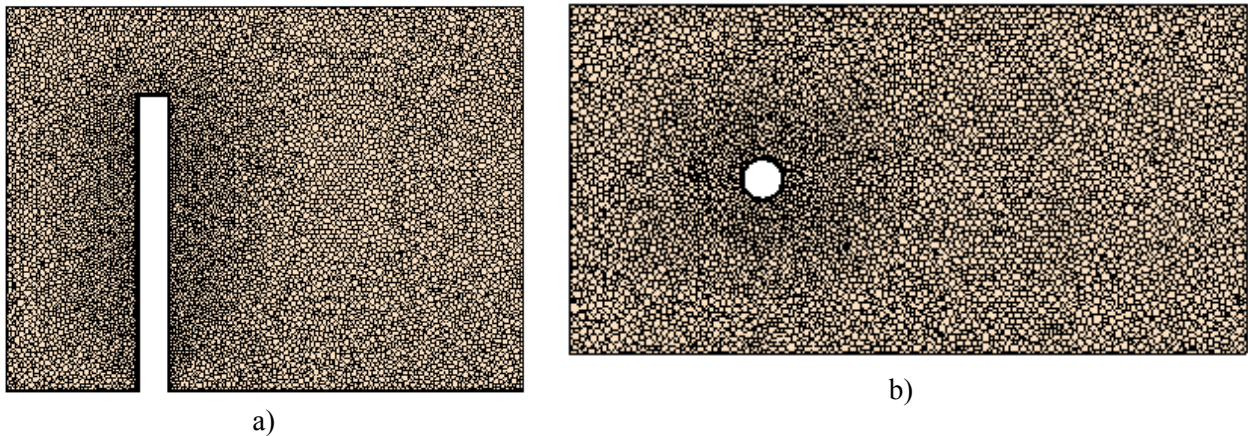


**Figure 2** The chosen mesh: a) at the plane of symmetry, b) top view at the cross-sectional plane

**Heat Transfer Case Description**

In this study, a constant temperature of 373.15 K is applied on the surface of the VG (RVG and FVG). In contrast, a 293.15 K (air) flow injected into the domain from the inlet. The material used for the FVG in this study is aluminium. The purpose of selecting aluminium is to simulate a real-life condition as metal is commonly used to conduct heat. Besides, it is also because the polymer materials used in the previous studies are technically poor in conducting heat, not to mention its low melting point that discourages its usage in the real application. However, even though aluminium; one of the softest metals is used, its Young's Modulus ( $E$ ) is still considered high. As a result,

from the heat source (due to the increased circulation discussed in previous), which improves the heat transfer rates. Note that all the boundary conditions in the RVG and FVG study will be exactly the same, except in the FVG study, the structural model will be activated to compute the FVG's motion.

Furthermore, the Nusselt Number ( $Nu$ ) and the temperature of the wake will be examined to justify the heat transfer performance. The  $Nu$  is used to quantify the heat transfer between a boundary (surface) and a fluid. It is the ratio of convective to conductive heat transfer across the boundary.

**RESULTS AND DISCUSSION**

Abbreviations will be provided to facilitate the following discussion. Using this abbreviation, the lengthy "AR=8 circular FVG" can be written as 8CF accordingly; where the "8" denotes the aspect ratio, the subscript "C-" denotes "circular" (it will be "P" for the flat plate), and the "F" denotes "FVG" (it will be "R" for RVG). With this concept, "AR=5 flat plate RVG" can be written as 5PR.

The computed  $\Gamma$  or strength of vortices of the circular FVG and RVG show that the FVG generates a larger vortex compared to its rigid cylinder, which is consistent with the earlier findings after the wall shear stress study in [3]. It might be due to a disturbance occurred between the vorticity feeding period and the shedding period of a vortex.

The  $\lambda_2$  criterion of [9] is applied to define the vortex boundary, as provided in Figure 3. It is observed that the vortex is "peeled off" from the FVG instead of following a normal shedding phenomenon. This shows that the typical vorticity feeding phase is disturbed. This finding suggests that the shedding phase plays a significant role in vortex formation and its strength.

Similar to the result of the circular case, the vortices formed from flat plate FVG are typically larger than those generated from the flat plate RVG. It is significant to highlight that two different  $\Gamma$  is computed in the case of 6PF, namely the  $\Gamma (+)$  and  $\Gamma (-)$ . The "positive" and "negative" signs represent the FVG's direction of motion when the measured vortex is shed, i.e. the sign of structural velocity,  $U_s$ . The "positive" in  $\Gamma (+)$  means that the measured vortex is shed when the

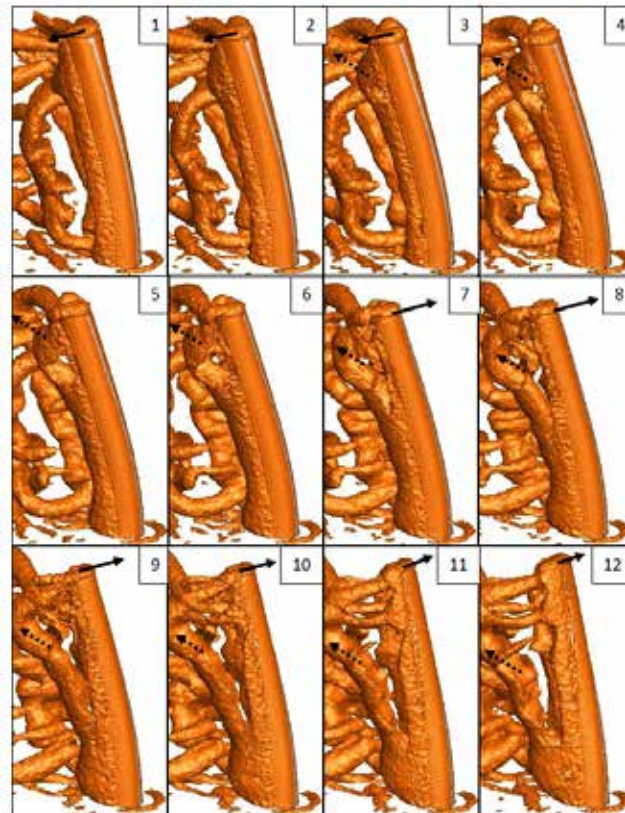


**Figure 3** Time series of the second eigenvalue – vortex forming and shedding, (1-3) vortex formation; (4-6) shedding of tip vortex, and (7-12) "peeling" of Kármán vortex. Dashed arrows denote the direction that the vortex tube/filament travels; solid arrows denote the direction that the circular FVG moves.

FVG is moving in the direction of the flow (i.e. +Us); while the “negative” in  $\Gamma$  (-) means otherwise (i.e., Us). According to the flow model proposed in the wall shear stress study of [3], the “negative” structural velocity (-Us) can enhance the shear rates and hence creating a larger vortex. This result shows that the prediction based on the proposed model is reliable, hence support the dependability of the model that is discussed in [3].

The proposed model in [3] also shows that the shear rate scales with the structural velocity. If the proposed model is consistent, the circulation should also scale with the structural velocity. To investigate this issue, the rms of the structural velocity is examined. The calculated results are given in Table 2 and Table 3. The structural velocity plots are shown for reference in Figures 4 and 5 for circular and flat plate FVGs, respectively. Based on the findings, the ascending sequence of the circulation generated by the circular FVG is 6CF, 10CF and 8CF, where the ascending sequence of the rms structural velocity is exactly similar, confirming that greater structural velocity leads to larger circulation. Similar behaviour is found in the flat plate case as well, as shown in Table 3.

This present study has demonstrated a different angle to study turbulence generation ability other than the classical statistical study. The spatial analysis provides the possibility to actively control the spatial scale of turbulence, without compromising the turbulence strength, by modifying the deflection of a VG in the system that has potential applications for vortex-induced vibration [10]-[15].

Figure 6 and 7 illustrate the mean Nusselt Number on the VGs’ front and a rear surface, respectively. On the front surface (Figure 6), the distribution and its magnitude are about the similar for both RVG and FVG cases, which suggests that the motion has a minimal effect to the mean Nusselt Number on the frontal surface. On the other hand, a distinct difference is observed between the mean Nusselt Number distributions on the rear surface between two cases, as shown in Figure 7. It can be clearly seen that, on the FVG’s rear surface, there is a region with greater mean Nusselt Number present near the free end when compared to the exact same spot of the RVG. The greater mean Nusselt Number denotes the surface experiences a greater heat transfer rate.

**Table 2** The normalized mean z-circulation ( $\Gamma_{z,FVG}$ ) at the highest considering plane and the normalized rms of structural velocity ( $U_{s,(rms)}$ ) associated to the 6<sub>CF</sub>, 8<sub>CF</sub> and 10<sub>CF</sub>

	$z/D$	$\Gamma_{z,FVG}/U_{\infty}D$ (negative)	$\Gamma_{z,FVG}/U_{\infty}D$ (positive)	$U_{s,y(rms)}/U_{\infty}$	$U_{s,x(rms)}/U_{\infty}$
6 <sub>CF</sub>	3	-7.85	7.61	±0.42	±0.13
8 <sub>CF</sub>	6	-8.29	8.86	±0.77	±0.17
10 <sub>CF</sub>	8	-7.94	8.04	±0.50	±0.14

**Table 3** The normalized mean z-circulation ( $\Gamma_{z,FVG}$ ) at the highest considering  $z/D$  and the normalized rms of structural velocity ( $U_{s,(rms)}$ ) associated with the 5<sub>PF</sub> and 6<sub>PF</sub>

	$z/D$	$-\Gamma_{z,FVG(-)}/U_{\infty}D$	$+\Gamma_{z,FVG(+)} / U_{\infty}D$	$U_{s,x(rms)}/U_{\infty}$	
5 <sub>PF</sub>	3	-12.45	12.28	±0.0086	
		$-\Gamma_{z,FVG(-)}/U_{\infty}D$	$-\Gamma_{z,FVG(+)} / U_{\infty}D$	$+\Gamma_{z,FVG(-)}/U_{\infty}D$	$+\Gamma_{z,FVG(+)} / U_{\infty}D$
6 <sub>PF</sub>	4	-17.18	-12.87	16.16	13.12
					±0.0414



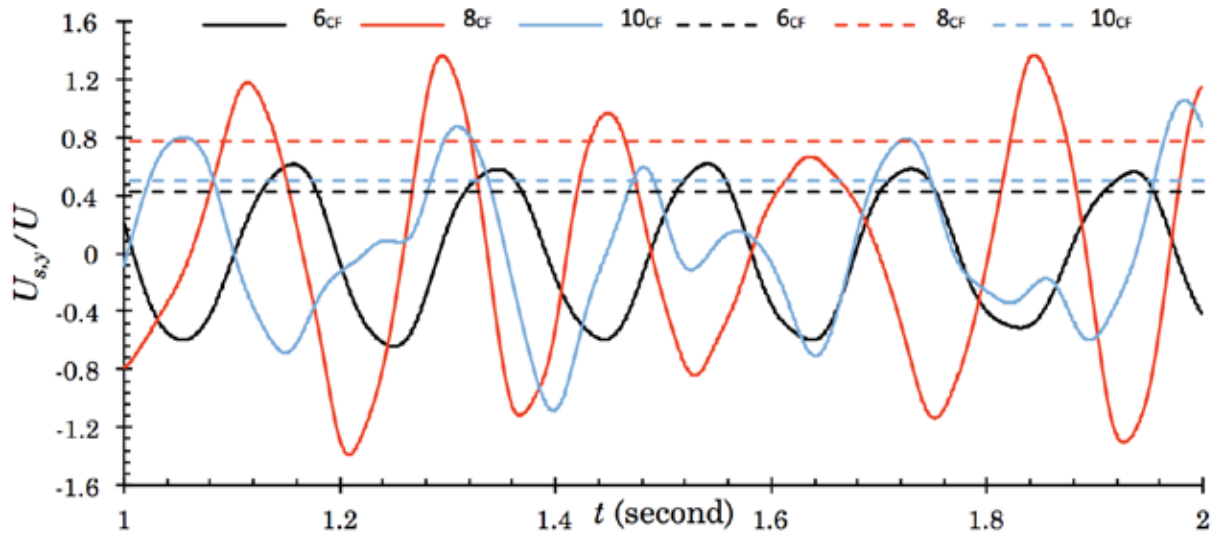


**Figure 4** The normalized structural velocity in the y-direction ( $U_{s,y}/U_{\infty}$ ) of the circular FVG with different AR. The solid line represents the instantaneous component; dash line represents its rms

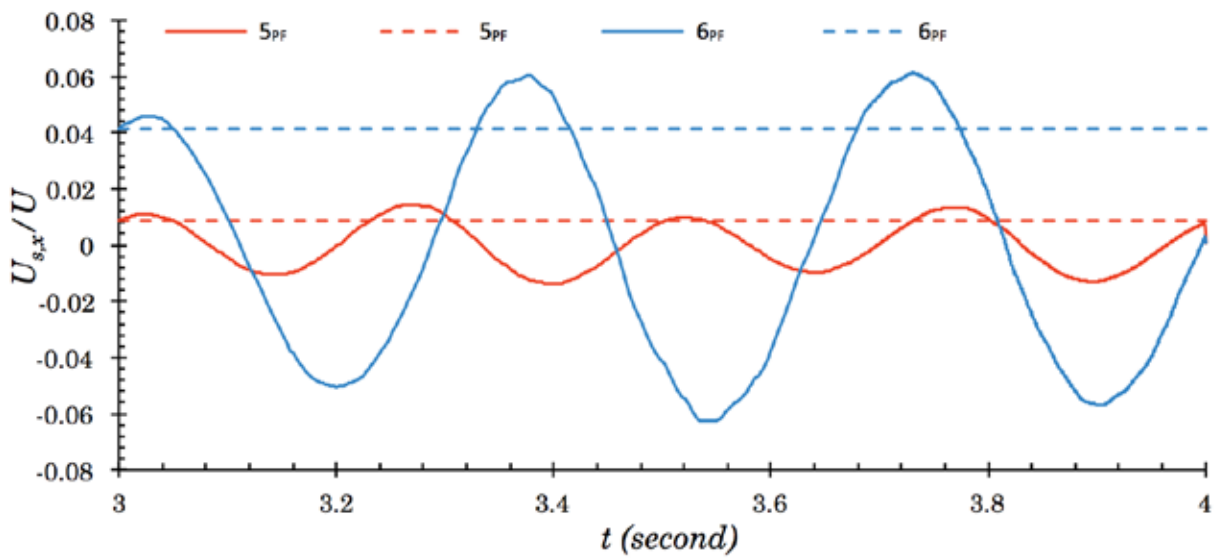


**Figure 5** The normalized structural velocity in the x-direction ( $U_{s,x}/U_{\infty}$ ) of the flat plate FVG with different AR. The solid line represents the instantaneous component; dash line represents its rms

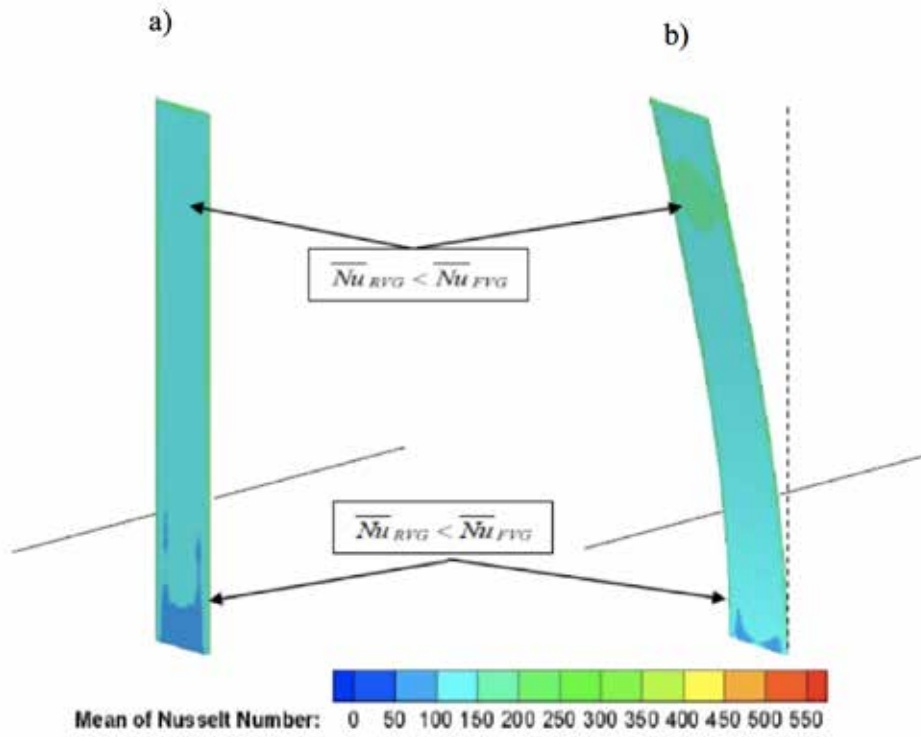


**Figure 6** Mean Nusselt Number on the frontal surface of the flat plate (a) RVG and (b) FVG

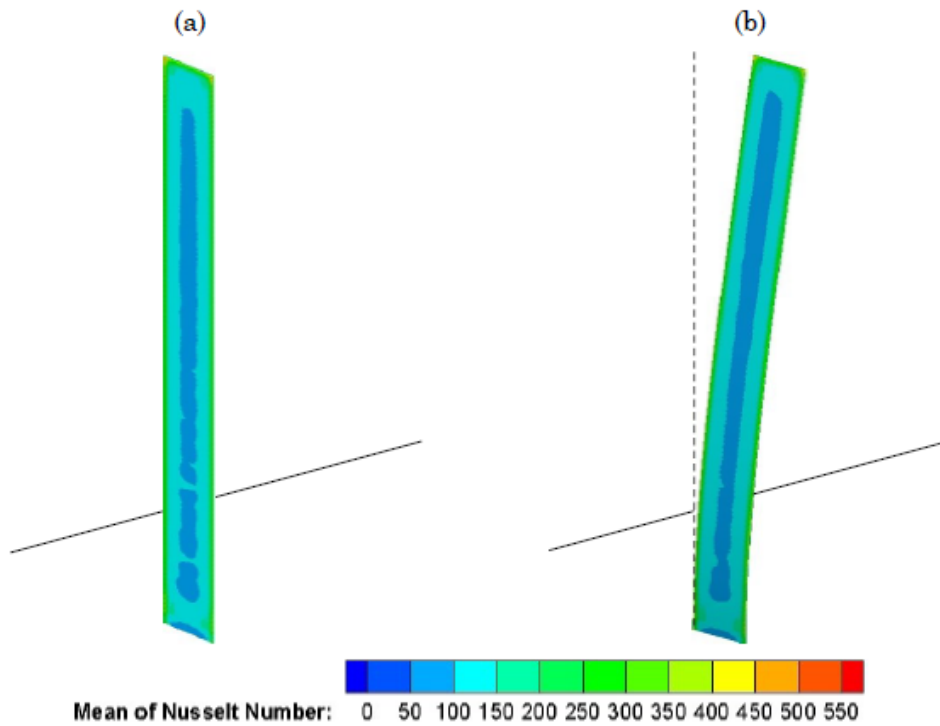


**Figure 7** Mean Nusselt Number on the rear surface of the flat plate (a) RVG and (b) FVG

Based on the wake visualization discussion presented earlier, it has been identified that the near wake flow behind an FVG experiences a distinctive change on its flow feature. Firstly, the downwash has become weaker, and secondly, the Karman vortex has grown stronger when an FVG is employed. Therefore, the changes in mean Nusselt Number distribution at the rear surface of the FVG can be attributed to the fact that the near wake flow behind the FVG has changed. Since it is known that the flow is responsible for the heat transfer, the greater mean Nusselt Number in the case of FVG suggests that the flow features behind the FVG favour the heat transfer process.

Furthermore, the increased mean Nusselt Number on the FVG's surface suggests that the wake behind the FVG, in particular, the vortex is carrying greater heat compared to the vortex in the case of RVG. According to the temperature profiles (Figure 8), the wake of FVG generally has a slightly greater temperature than the RVG's wake. It can be seen that the temperature at the immediate downstream of the RVG is a lot greater than that of the FVG. The contour shows that the heat is trapped behind the RVG, probably due to the existence of the stronger downwash as discussed previously, which leads to the formation of the observed high-temperature region.

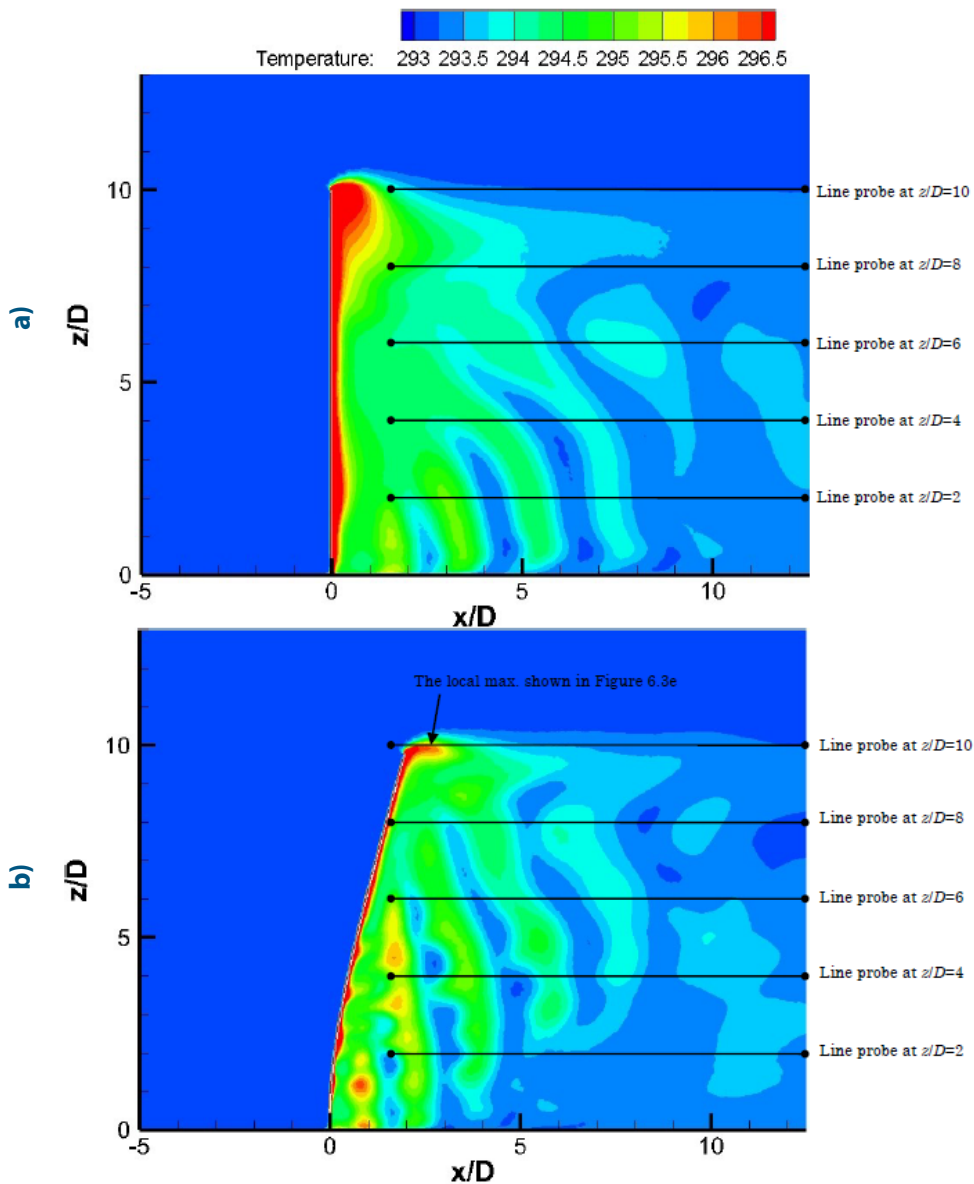


**Figure 8** Temperature contour at the plane of symmetry ( $y=0$ ) of the a) RVG and b) FVG



Since the formed vortex is responsible for carrying the heat away from this region, the result has directly demonstrated that the vortex generated from the RVG is ineffective in conveying the trapped heat to the remaining fluid region. This argument can also be supported by the fact that the vortex behind the RVG is carrying less heat (has a lower temperature) than the vortex behind the FVG. Once again, the results have strongly evidenced the important role of the vortex in transporting heat from the VG to the flow. Relating the observations from this study with the earlier findings, it is believed that a stronger vortex is beneficial to transporting heat from the heated VG to the flow. In other words, the FVG is indeed performing better in heat transfer due to the stronger vortex generated from it.

Then the heat source is applied on the ground plate where the VG is placed. This is a common configuration used in the study of VG-induced heat transfer enhancement, including the Shape Memory Alloy VG study conducted by Aris et al. [16]. For this purpose, both mean Nusselt Number and temperature profiles are examined to study the heat transfer performance of the case. However, the findings from both analyses have demonstrated a different conclusion. Firstly, based on the Nusselt Number contour, the RVG case is said to have an overall better heat transfer performance.

On the contrary, the temperature profiles show that the FVG provides a better heat transfer at its downstream. However, if the ultimate goal of the heat

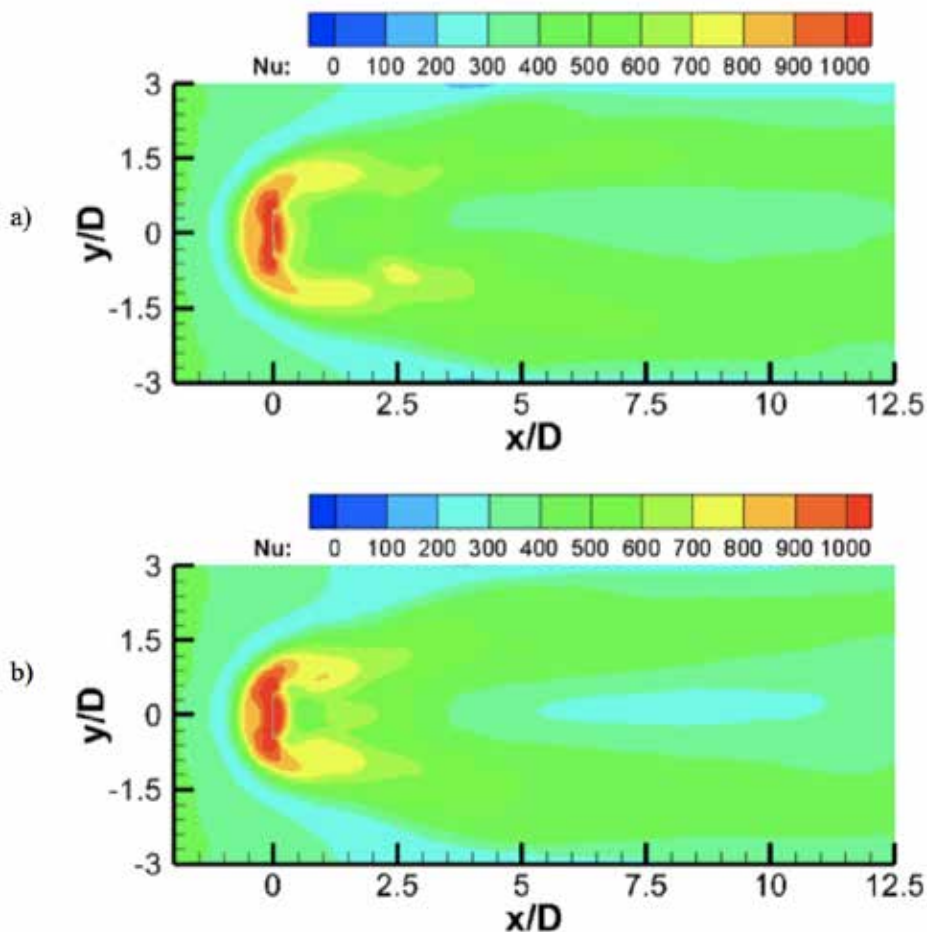


Figure 9 The mean Nusselt Number on the ground plate of a) the RVG, b) FVG

transfer process is to deliver the heat up the fluid that flows in the system, then the FVG can be considered to have a better heat transfer performance.

In addition, to the authors' opinion, the heat transfer performance at further downstream does not actually play a significant role in the actual application of the FVG. As commonly known, a heat transfer system is regularly featuring multiple VGs that are arranged in a certain order and/or configuration [17]-[18]. In other words, the effective region that a single FVG has to take care will be the region around it, before the subsequent FVG overtakes the responsibility. Since the  $Nu$  around the FVG is higher than that of the RVG, the FVG allows a relatively efficient heating process at its immediate downstream. Thus, it is preferred than the RVG. Figure 9 of the mean Nusselt Number confirms these findings. At the region around the VG, it can be seen that the heat transfer rate around the FVG is greater than that of the RVG in term of its spatial distribution. Therefore, it can be said that the FVG has promoted the heat transfer rate and hence, lead to a better heat transfer performance.

## CONCLUSION

Based on the results, it can be concluded that the FVG has an enhanced turbulence production ability compared to its respective rigid counterpart. The physics of this phenomenon that has been lacking from the previous studies has also been answered. It was observed that the proposed flow model could potentially provide a universal description to any similar phenomenon (e.g. vortex strength, turbulence production, and shear layer physics) for any submerged structure (with any geometries and shapes) that is in motions, including rotational motion.

The work has also demonstrated the heat transfer performance of the proposed FVG. Comparisons with the typical RVG system are made to justify its performance. First of all, it has been identified that the strength of vortex has played a crucial role in heat transfer. Based on the result, a stronger vortex will draw more heat from the heated VG resulting in a better heat transfer process. As a result, the flow temperature behind the FVG is higher than the flow behind the RVG. Although the mean Nusselt Number contour shows that the RVG has an overall greater heat transfer rate, it is later identified that the result is caused by the fact that the flow temperature at far downstream of the FVG is greater than that of the RVG case. Due to the decreasing temperature difference between the heated surface and the flow, the Nusselt Number in the case of FVG shows a lower value than the RVG case. However, since the goal of the heat transfer process is to heat the flow, the FVG is positively performing better than the RVG.

In overall, the results have shown that FVG performs better than the RVG in term of conveying heat to the flow. Although the improvement may be small as shown from the result, the total improvement when multiple FVGs are employed (i.e. which is a common practice in the actual application) can be significant. Besides, this study has considered only a fraction of the full potential of an FVG. Further studies are required to explore the effects and impacts of employing an FVG or an array of FVGs on heat transfer system.

## ACKNOWLEDGEMENT

This research project was fully supported and funded by the Fundamental Research Grant Scheme FRGS 1/2013 from the Ministry of Higher Education Malaysia.

**REFERENCES**

- [1] H.B. Chan, H.Y. Tshun, P. Kumar, K.W. Siaw & S.S. Dol, "The Numerical Investigation on the Effects of Aspect Ratio and Cross-Sectional Shape on the Wake Structure Behind a Cantilever", *Journal of Engineering and Applied Sciences*, 11, 16, pp. 9922-932, 2016.
- [2] T.H. Yong, H.B. Chan, S.S. Dol, S.K. Wee & P. Kumar, "The flow dynamics behind a flexible finite cylinder as a flexible agitator", In *IOP Conference Series: Materials Science and Engineering*, 206, p. 012033, 2017.
- [3] S.S. Dol, S.K. Wee, H.B. Chan & P. Kumar, "Turbulence characteristics behind a flexible vortex generator", *WSEAS Transaction on Fluid Mechanics*, 14, pp. 1-7, 2019.
- [4] S.S. Dol, M.M. Salek & R.J. Martinuzzi, "Effects of pulsation to the mean-field and vortex development in a backwards-facing step flow", *Journal of Fluids Engineering*, 136, 1, 2014. Doi: 10.1115/1.4025608
- [5] S.S. Dol, M.M. Salek & R.J. Martinuzzi, "Energy redistribution between the mean and pulsating flow field in a separated flow region", *Journal of Fluids Engineering*, 136, 11, pp. 111105-1-9, 2014.
- [6] S.S. Dol, G.A. Kopp & R.J. Martinuzzi, "The suppression of periodic vortex shedding from a rotating circular cylinder", *Journal of Wind Engineering and Industrial Aerodynamics*, 96, 6, pp. 1164-184, 2008.
- [7] M.M. Salek, S.S. Dol & R.J. Martinuzzi, "Analysis of pulsatile flow in a separated flow region", in *ASME 2009 Fluids Engineering Division Summer Meeting*, pp. 1429-1438, 2009.
- [8] F.B. Tian, H. Dai, H. Luo, J.F. Doyle & B. Rousseau. "Fluid-structure interaction involving large deformations: 3D simulations and applications to biological systems", *Journal of Computational Physics*, 258, pp. 451-469, 2014.
- [9] J. Jeong & H. Fazle, "On the identification of a vortex", *Journal of Fluid Mechanics*, 285, pp. 69-94, 1995.
- [10] M.A. Zahari & S.S. Dol, "Alternative energy using vortex-induced vibration from turbulent flows: Theoretical and analytical analysis", *IET*, pp. 1-16, 2014.
- [11] M.A. Zahari & S.S. Dol, "Effects of different sizes of cylinder diameter on vortex-induced vibration for energy generation", *Journal of Applied Sciences* 15, 5, pp. 783-791, 2015.
- [12] M. Zahari, H. B. Chan, T. H. Yong & S. S. Dol, "The effects of spring stiffness on vortex-induced vibration for energy generation", in *IOP Conference Series: Materials Science and Engineering*, Vol. 78, No. 1, p. 012041, 2015.
- [13] T.Y. Khing, M.A. Zahari & S. S. Dol, "Application of vortex-induced vibration energy generation technologies to the offshore oil and gas platform: The feasibility study. World Academy of Science, Engineering and Technology", *International Journal of Mechanical, Aerospace, Industrial, Mechatronic and Manufacturing Engineering*, 9, 4, pp. 661-666, 2015.
- [14] C.W. Park & S.J. Lee, "Free end effects on the near wake flow structure behind a finite circular cylinder", *Journal of Wind Engineering and Industrial Aerodynamics* 88, 2, pp. 231-246, 2000.

- [15] K.M. Lam, P. Liu & J.C. Hu. "Combined action of transverse oscillations and uniform cross-flow on vortex formation and pattern of a circular cylinder", *Journal of Fluids and Structures* 26, 5, pp. 703-721, 2010.
- [16] M.S. Aris, I. Owen & C.J. Sutcliffe, "The application of shape memory alloy as vortex generators and flow control devices for enhanced convective heat transfer", in *ASME/JSME 2007 5th Joint Fluids Engineering Conference, American Society of Mechanical Engineers*, pp. 1465-470, 2007.
- [17] A.A. Azeez, S.S. Dol & S.K. Mohammad, "Effects of cylinder shape on the performance of vortex-induced vibration for aquatic renewable energy", in *2019 Advances in Science and Engineering Technology International Conferences (ASET)*, pp. 1-4, 2019.
- [18] M.A. Zahari & S.S. Dol, "Application of vortex-induced vibration energy generation technologies to the offshore oil and gas platform: The preliminary study", *International Journal of World Academy of Science, Engineering and Technology* 8, 7, pp. 1331-334, 2014.